

# **Supporting information: Two-stage photodegradation of indomethacin molecular nanocomposites under extreme confinement**


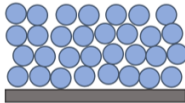
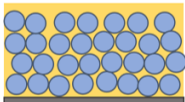
Cindy Yueli Chen,<sup>†</sup> Haonan Wang,<sup>‡</sup> Ahmad Arabi Shamsabadi,<sup>†</sup> and Zahra  
Fakhraai<sup>\*,†</sup>

*<sup>†</sup>Department of Chemistry, University of Pennsylvania, Philadelphia, Pennsylvania 19104,  
United States*

*<sup>‡</sup>Corning Research Center, Shanghai 201206, China*

E-mail: fakhraai@sas.upenn.edu

Table S1: The Cauchy model ( $n = A + \frac{B}{\lambda^2}$ ) was employed to accurately fit the optical properties of a pure IMC film (top row), a porous nanoparticle (NP) film made by 25 nm NPs after sintering at 773 K for 30 mins (middle row), and an IMC/SiO<sub>2</sub>(25 nm) MNCF after infiltration (bottom row). For the MNCF, two Cauchy layers were considered, one for the nanocomposite layer and one for the top residual IMC layer. The thickness of the nanocomposite layer and the index of refraction of the residual IMC layer were held constant to avoid overfitting. The index of refraction of the residual IMC was determined from the bulk IMC film (top row). In each row, the schematic geometry of the film is shown on the left, the ellipsometry fitting details are shown in the middle, and the final calculated values of the thickness and index of refraction are shown on the right. Parameters shown in bold were fitted variables. Mean square error (MSE) describes the goodness of the fit to the ellipsometric angles  $\Psi(\lambda)$  and  $\Delta(\lambda)$ .

	SE Model	Fitting results
<p><b>IMC</b></p> 	<p>Layer # 2 = <b>Cauchy</b> Thickness # 2 = <b>77.58 nm</b> (fit)  A = <b>1.590</b> (fit) B = <b>0.01402</b> (fit) C = <b>0.0000</b>  + <b>Urbach Absorption Parameters</b>  Layer # 1 = <b>NTVE_JAW</b> Native Oxide = <b>1.00 nm</b>  Substrate = <b>Si_JAW</b></p>	<p>MSE = 0.771  Thickness #2 = 77.6 ± 0.0  n of IMC = 1.624 ± 0.005</p>
<p><b>NP film (25 nm NPs)</b></p> 	<p>Layer # 2 = <b>Cauchy</b> Thickness # 2 = <b>195.34 nm</b> (fit)  A = <b>1.277</b> (fit) B = <b>0.00368</b> (fit) C = <b>0.0000</b>  + <b>Urbach Absorption Parameters</b>  Layer # 1 = <b>NTVE_JAW</b> Native Oxide = <b>1.00 nm</b>  Substrate = <b>Si_JAW</b></p>	<p>MSE = 4.072  Thickness #2 = 195.3 ± 0.0  n of NP = 1.287 ± 0.005</p>
<p><b>IMC/SiO<sub>2</sub>(25 nm) (after IMC infiltration)</b></p> 	<p>Layer # 3 = <b>Cauchy</b> Thickness # 3 = <b>3.10 nm</b> (fit)  A = <b>1.590</b> B = <b>0.01402</b> C = <b>0.0000</b>  + <b>Urbach Absorption Parameters</b>  Layer # 2 = <b>Cauchy</b> Thickness # 2 = <b>195.34 nm</b>  A = <b>1.492</b> (fit) B = <b>0.00947</b> (fit) C = <b>0.0000</b>  + <b>Urbach Absorption Parameters</b>  Layer # 1 = <b>INTR_JAW</b> Thickness # 1 = <b>1.00 nm</b>  Substrate = <b>Si_JAW</b></p>	<p>MSE = 3.214  Thickness #3 = 3.1 ± 0.0  n of NP = 1.516 ± 0.005</p>

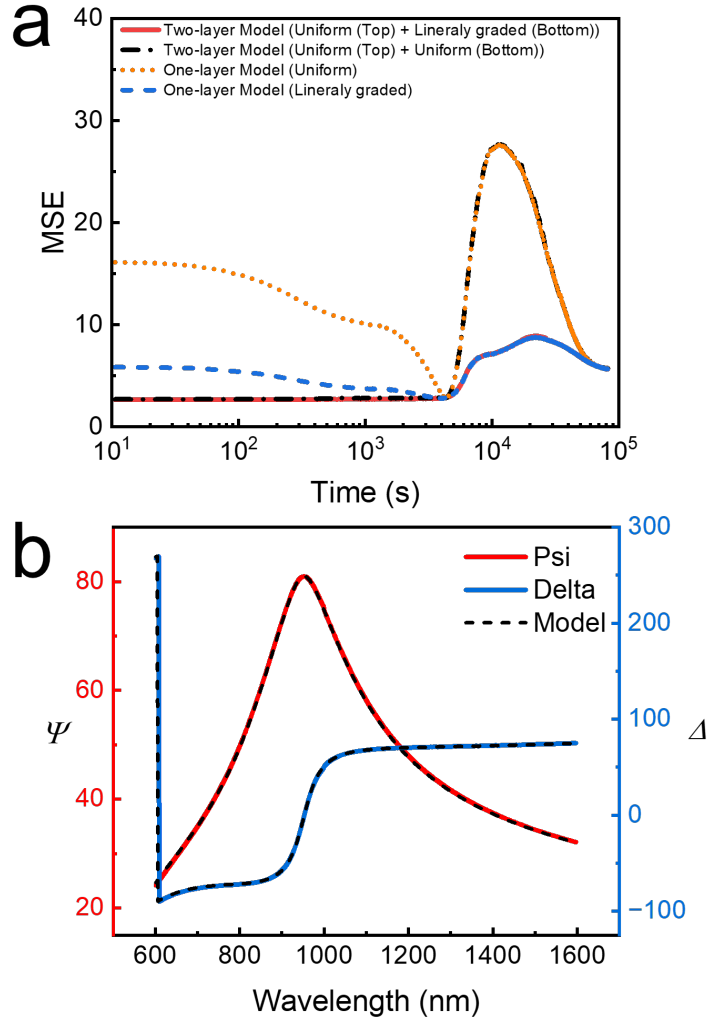


Figure S1: (a) The mean square error (MSE) of various fitting models for an IMC/SiO<sub>2</sub>(25 nm) MNCF with a residual IMC top layer. Four different models were employed to fit the data. The two-layer models include an IMC layer (top) in addition to the nanocomposite layer (bottom). The two-layer models (black short dash dots for the uniform model and red solid line for the linearly-graded model) fit the data better during the Stage 1 photodegradation ( $< 3 \times 10^3$  s). The equal and low MSE values observed between the graded and uniform fittings obtained from the two-layer model suggest that the degradation of the nanocomposite layer is evenly distributed across the entire nanocomposite layer. During Stage 2, where the top IMC layer is fully degraded ( $> 4 \times 10^3$  s), the linearly graded models (blue short dash for the one-layer model and red solid line for the two-layer model) have significantly lower MSE values. (b) Ellipsometric angles  $\Psi$  (red) and  $\Delta$  (blue) vs. wavelength for an IMC/SiO<sub>2</sub>(25 nm) film. The wavelength range of  $600 < \lambda < 1600$  nm was used to fit the data in the transparent region of the IMC spectrum. The dashed line shows the fit to the one-layer linearly-graded model at the beginning of UV exposure. While the two-layer graded model (red solid line in (a) better captures the film properties for the entire duration of the experiments, the one-layer graded model (blue short dashed line in (a) and black dashed line in (b)) provides a reasonable fit without additional fitting parameters.

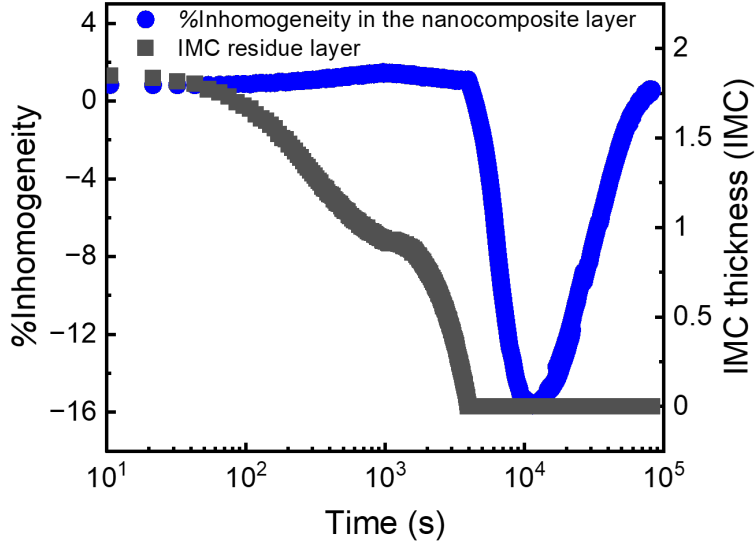


Figure S2: %Inhomogeneity (blue, circle) in the nanocomposite layer and thickness of IMC residue layer (black, square) as a function of UV (254 nm) irradiation time for an IMC/SiO<sub>2</sub>(25 nm) MNCF. During Stage 1 of photodegradation ( $< 3 \times 10^3$  s), the top layer thickness decreases, showing the degradation of the top layer. %inhomogeneity in the nanocomposite remains nearly constant, indicating a uniform degradation process throughout the entire nanocomposite layer. During the Stage 2 photodegradation ( $> 4 \times 10^3$  s), %inhomogeneity shows a rapid non-monotonic change, with lower values of the refractive index near the free surface, indicating faster degradation of the surface region.<sup>1</sup>

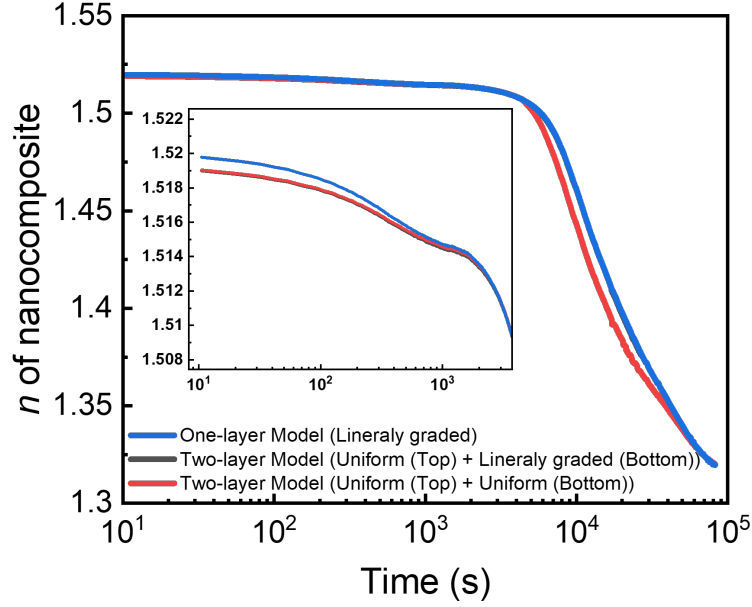


Figure S3: Refractive index ( $n$ ) of the nanocomposite layer as a function of UV (254 nm) irradiation time for an IMC/SiO<sub>2</sub> film. The results were fitted using three different models: a two-layer model with two uniform layers accounting for the nanocomposite layer (bottom) and the top IMC residual layer (red), a two-layer model where a linearly-graded model is used to fit the bottom nanocomposite layer (black) and a one-layer linearly-graded model, assuming the top residual layer is negligible (blue). For linearly-graded models,  $n$  represents the index of refraction at the film center. All three models result in similar values of  $n$  for the duration of the experiment. The inset shows a zoomed version of the Stage 1 photodegradation, revealing a mere 0.001 difference in the fitted refractive index values between the one-layer and two-layer models, which is within the instrument accuracy of 0.005.

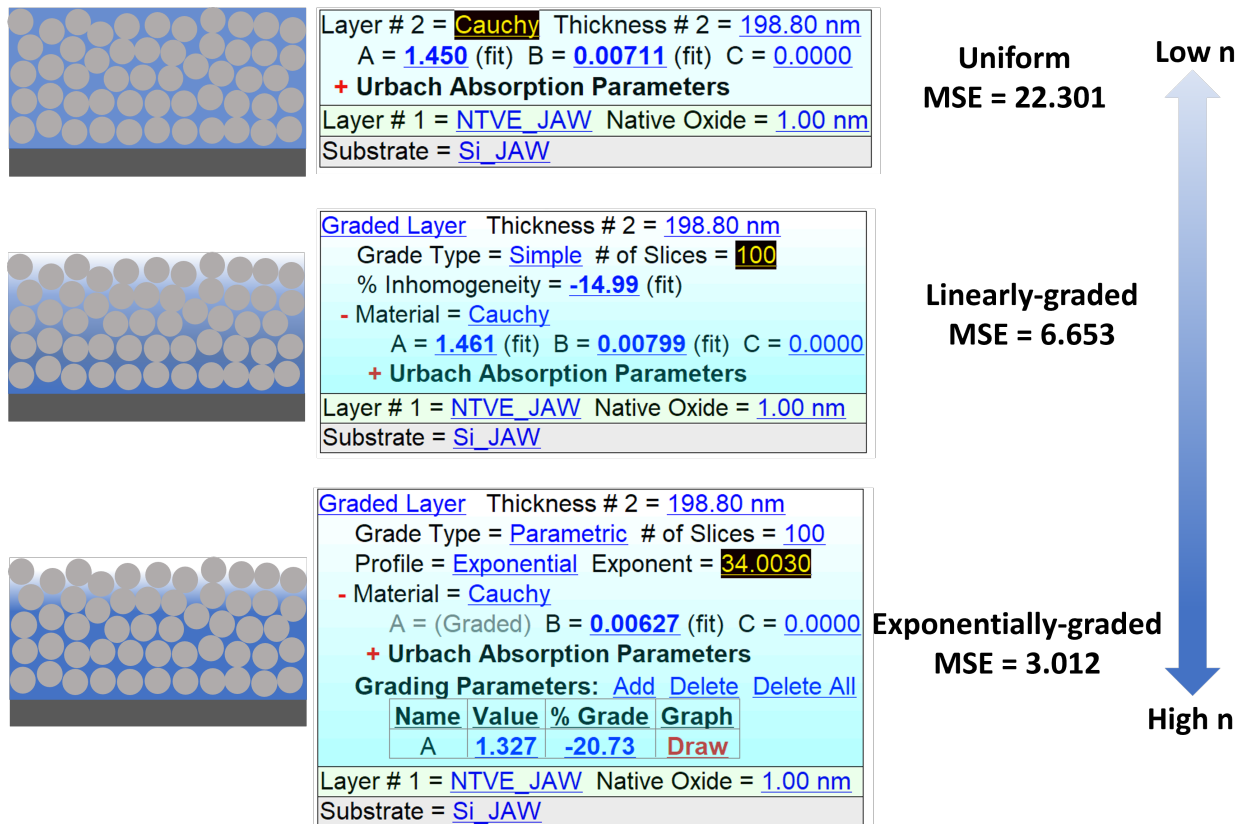


Figure S4: Comparison between different SE models used to fit the data obtained for a  $\sim 200$  nm IMC/SiO<sub>2</sub>(25 nm) layer exposed to 254 nm UV light for  $9 \times 10^3$  s (15 % IMC mass loss, during the Stage 2 photodegradation) in ambient conditions. The left, middle, and right columns schematically show the properties of the assumed model, the corresponding SE models used to fit the data, and the mean square error of the fits, respectively. The arrow highlights the direction of inhomogeneity of the index of refraction ( $n$ ) in the linearly- and exponentially-graded models. Variables in bold were fitted, while other variables were held constant with time.

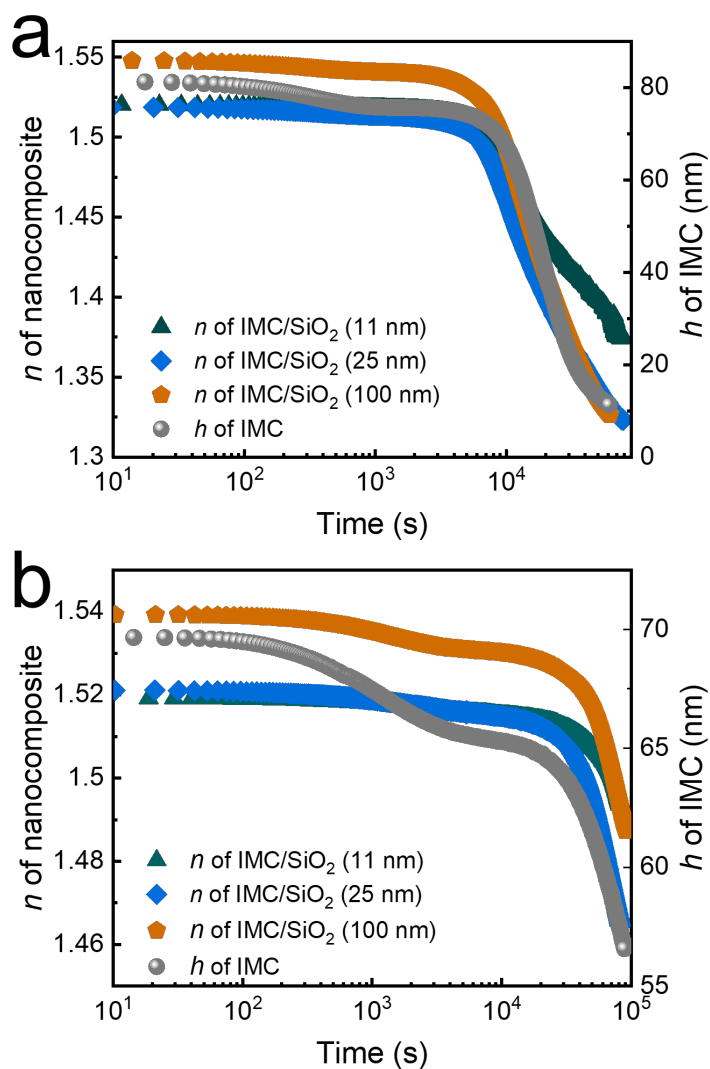


Figure S5: Refractive index of  $\sim 200$  nm IMC/SiO<sub>2</sub> nanocomposite films prepared from IMC and various NP diameters (left axis), and thickness of a pure IMC film (right axis) as a function of UV irradiation time at UV wavelengths of (a) 254 nm and (b) 365 nm.

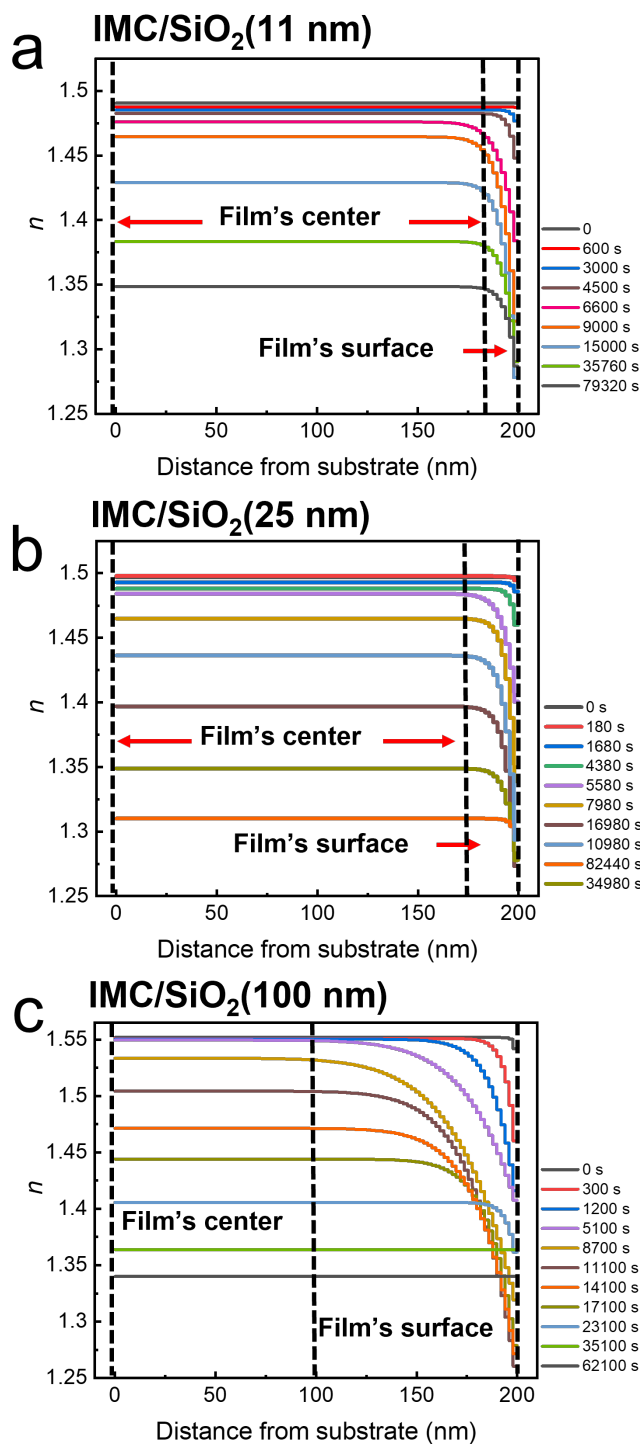


Figure S6: The refractive index profiles of  $\sim 200$  nm (a) IMC/SiO<sub>2</sub>(11 nm) (b) IMC/SiO<sub>2</sub>(25 nm), and (c) IMC/SiO<sub>2</sub>(100 nm) nanocomposite layers fitted using the exponentially-graded model.  $n$  is plotted as a function of distance from the substrate at various times during UV irradiation at 254 nm in ambient conditions. The red arrows show the film surface region, which is roughly equal to the diameter of the NP in each MNCF.



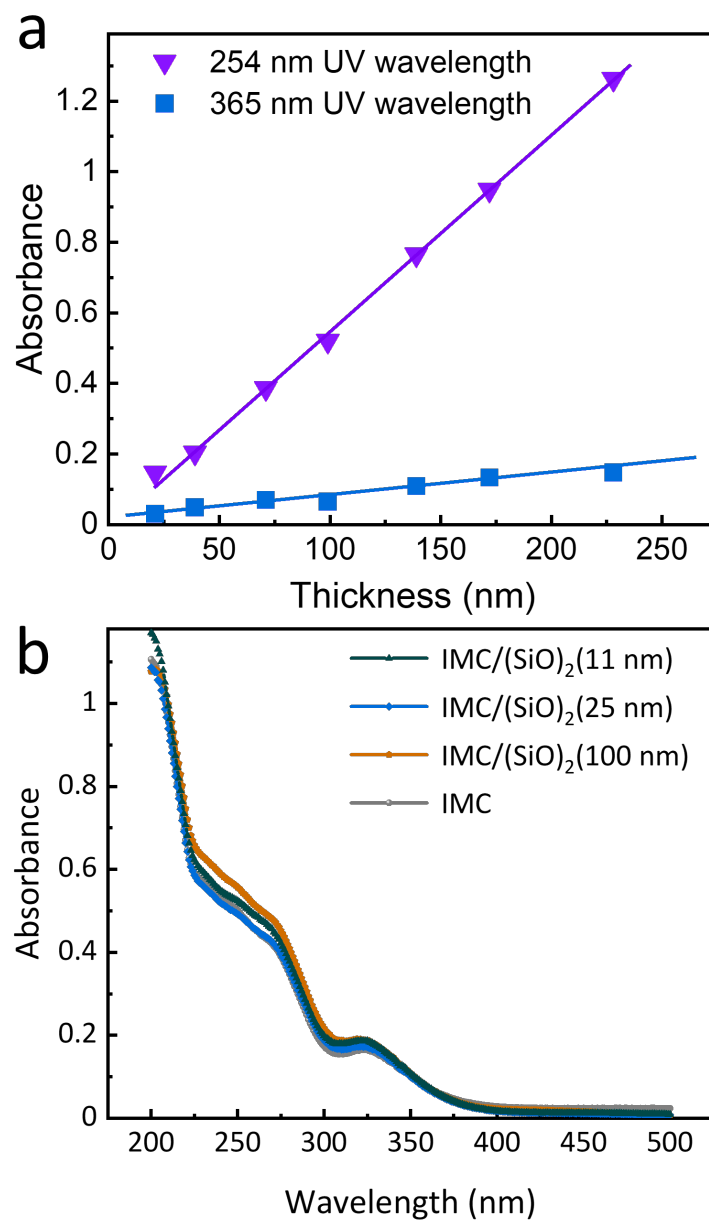


Figure S7: (a) UV-Vis absorbance as a function of IMC film thickness at the UV wavelengths of 254 nm (purple triangles) and 365 nm (blue squares). (b) Absorbance as a function of wavelength for a  $\sim 70$  nm IMC film (gray circles) compared with  $\sim 200$  nm MNCFs of IMC/SiO<sub>2</sub>(11 nm) (green triangles), IMC/SiO<sub>2</sub>(25 nm) (blue diamonds), and IMC/SiO<sub>2</sub>(100 nm) (orange pentagons). A  $\sim 200$  nm MNCF contains an equivalent IMC mass as  $\sim 70$  nm IMC film. The similar degree of absorbance in these films shows that the IMC mass (or thickness since the exposure area is the same) controls the degree of absorbance in the MNCFs, the contribution from silica NPs are negligible.

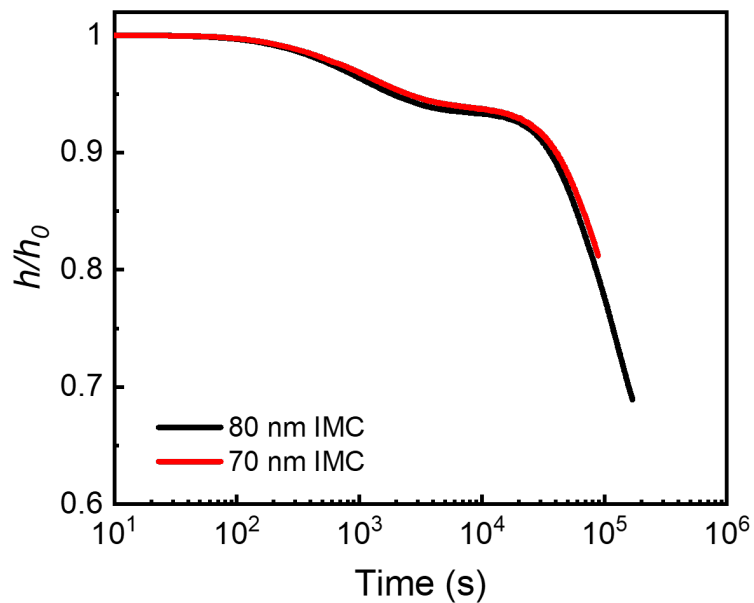
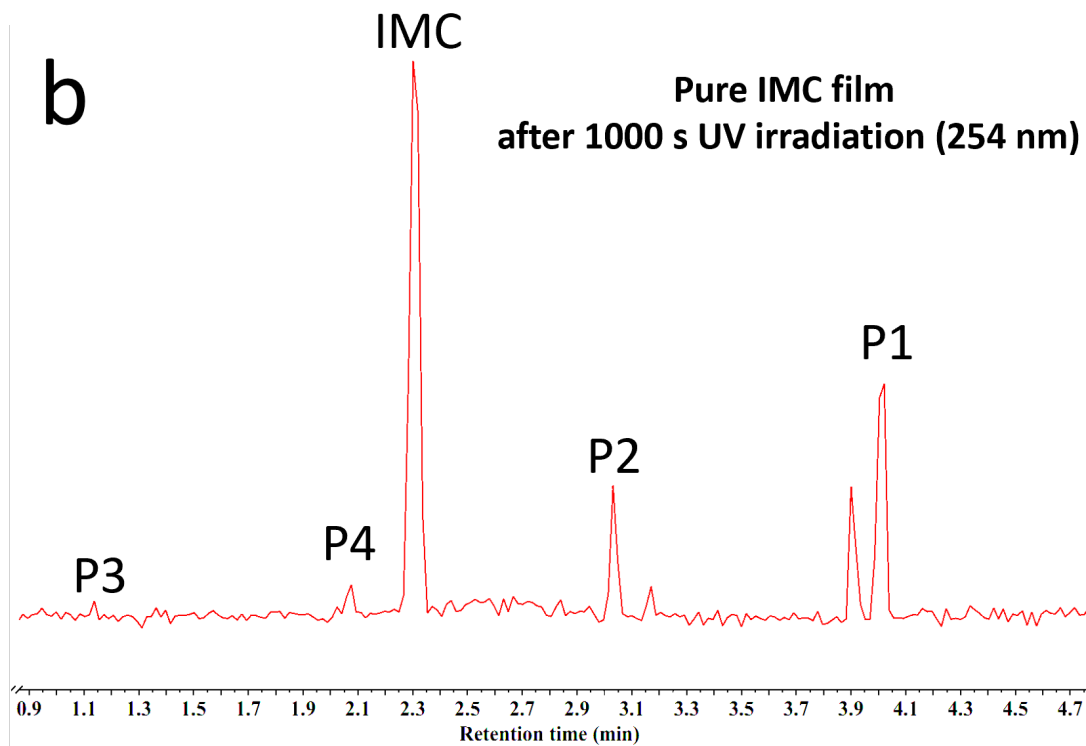
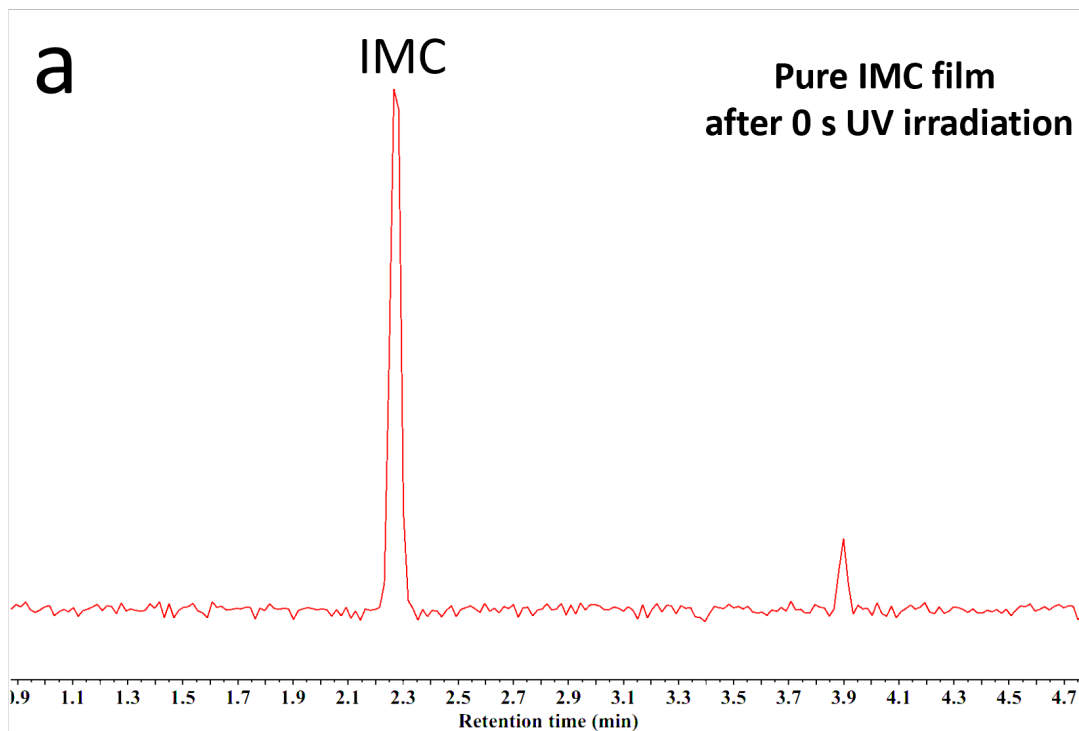


Figure S8: Photodegradation of 70 nm (red) and 80 nm (black) films of pure IMC in ambient conditions, measured as the relative change in the film thickness ( $h/h_0$ ) vs. 365 nm UV irradiation time.



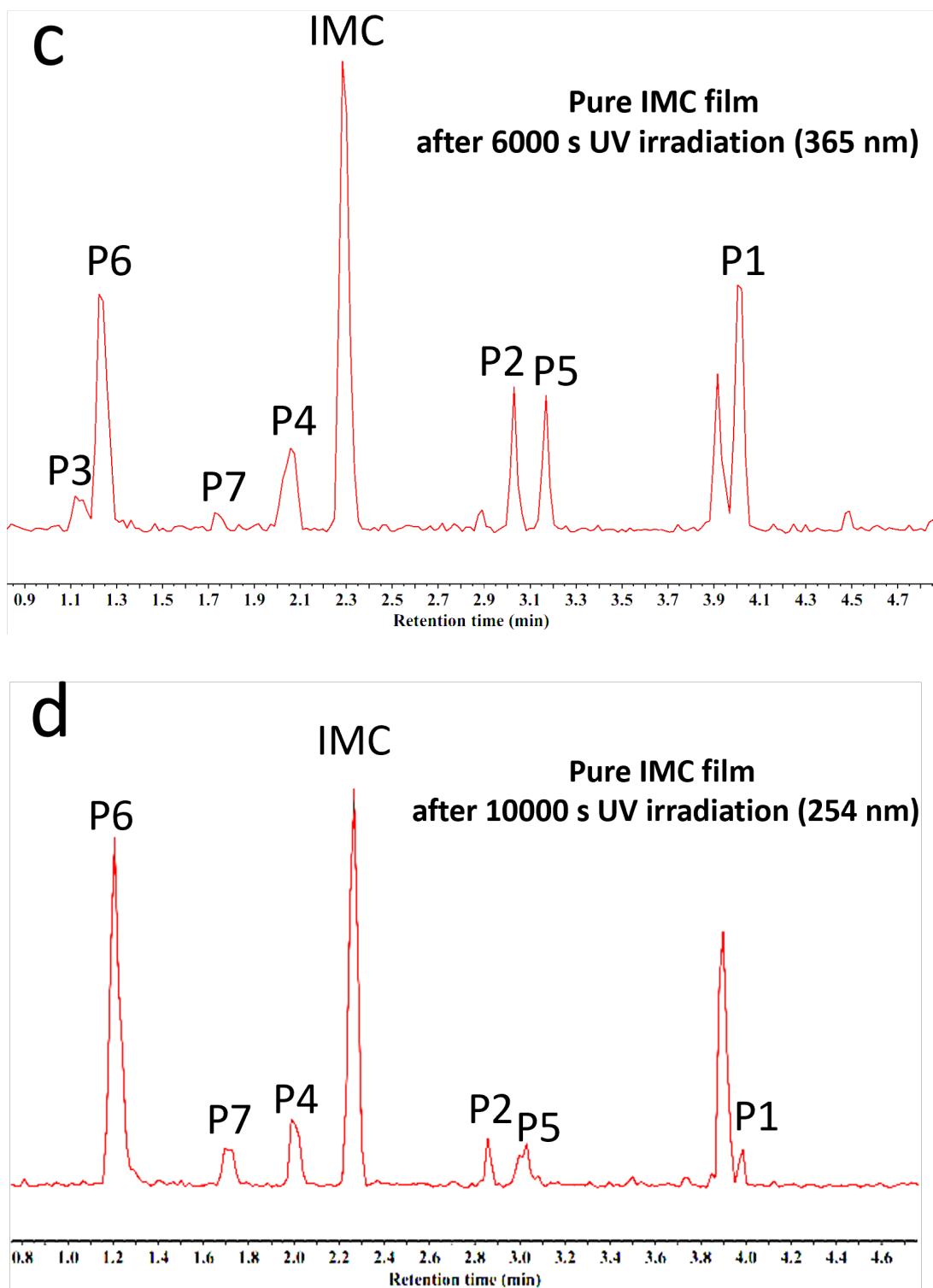
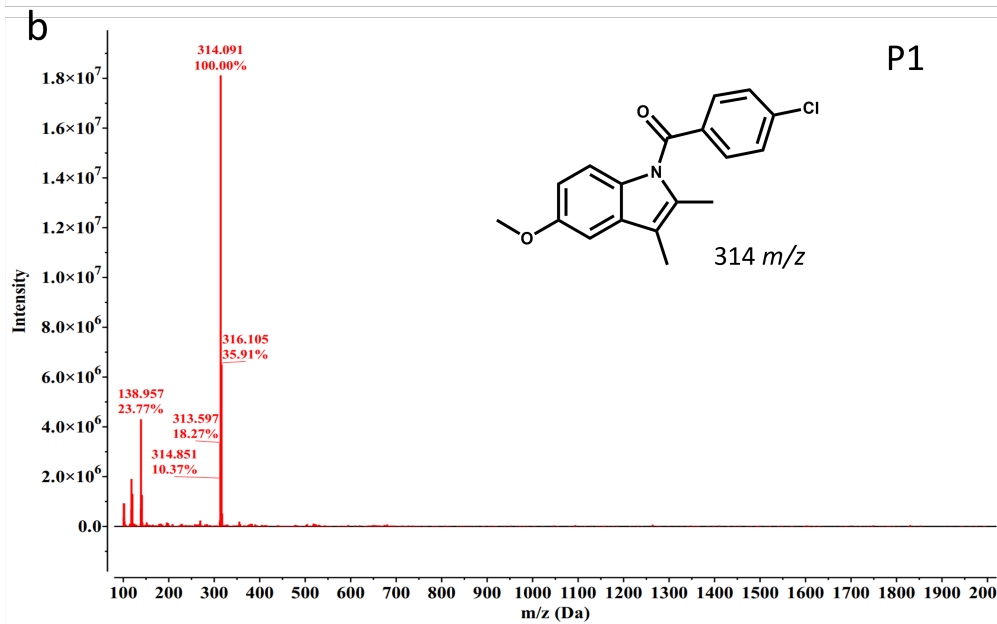
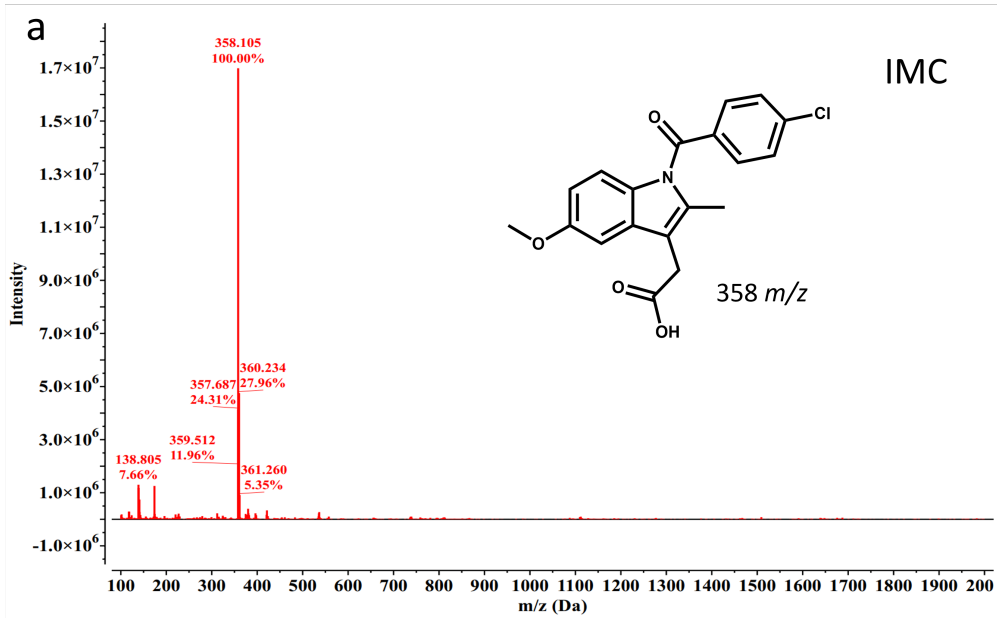
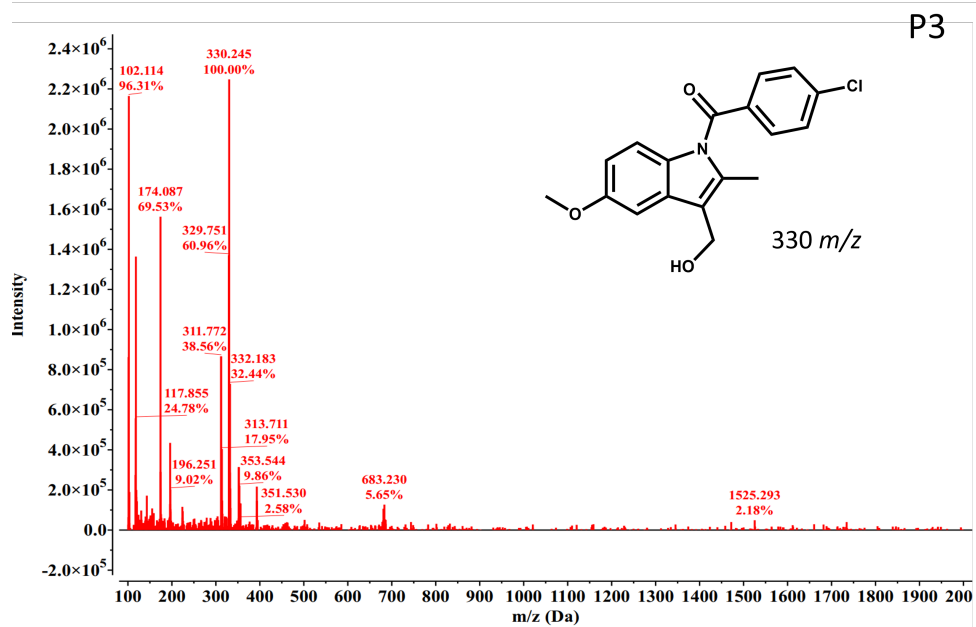
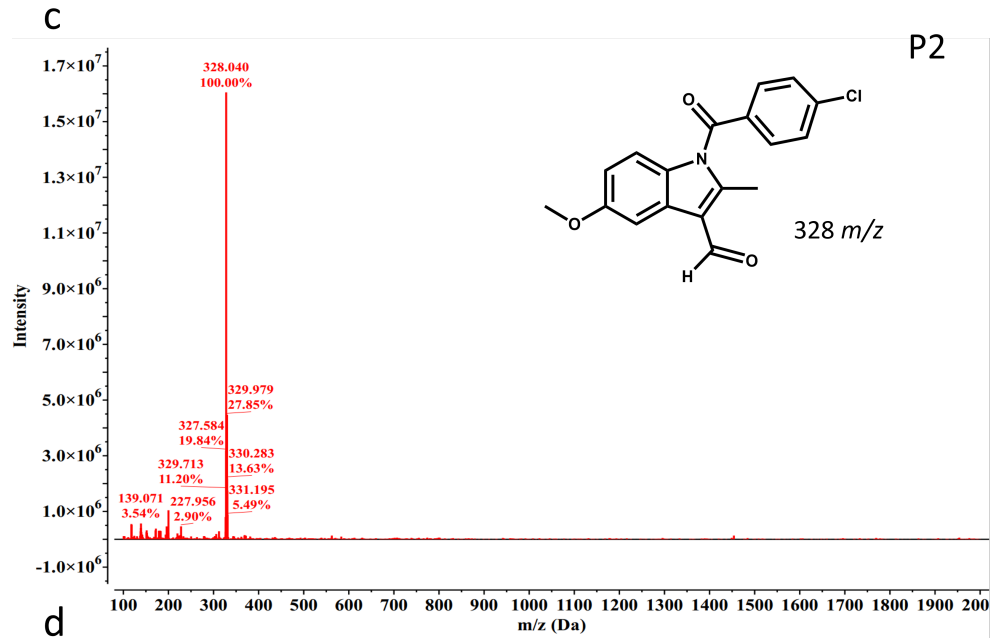
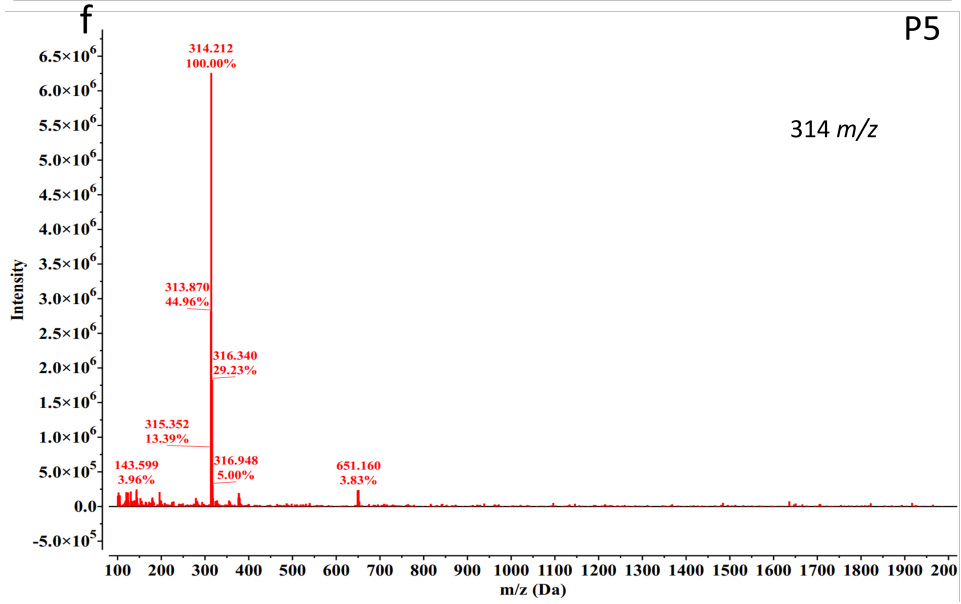
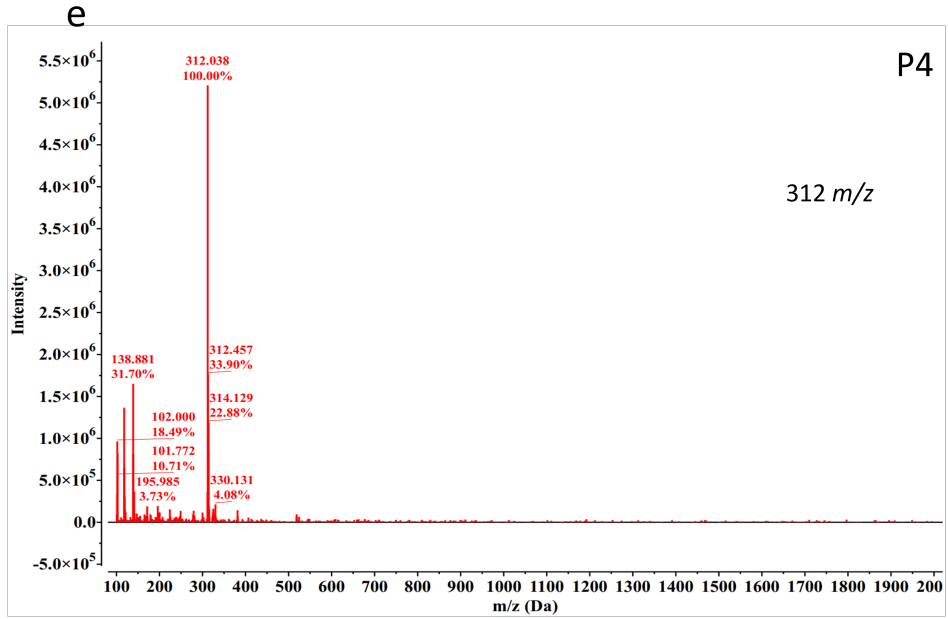


Figure S9: Representative total base peak UPLC chromatograms of mixtures of IMC removed from substrates in H<sub>2</sub>O/MeCN: (a) before UV irradiation, (b) after 1000 s of UV (254 nm) irradiation (Stage 1), (c) after  $6 \times 10^3$  s of UV (365 nm) irradiation (Stage 1), and (d) after  $10^4$  s of UV (254 nm) irradiation (Stage 2).







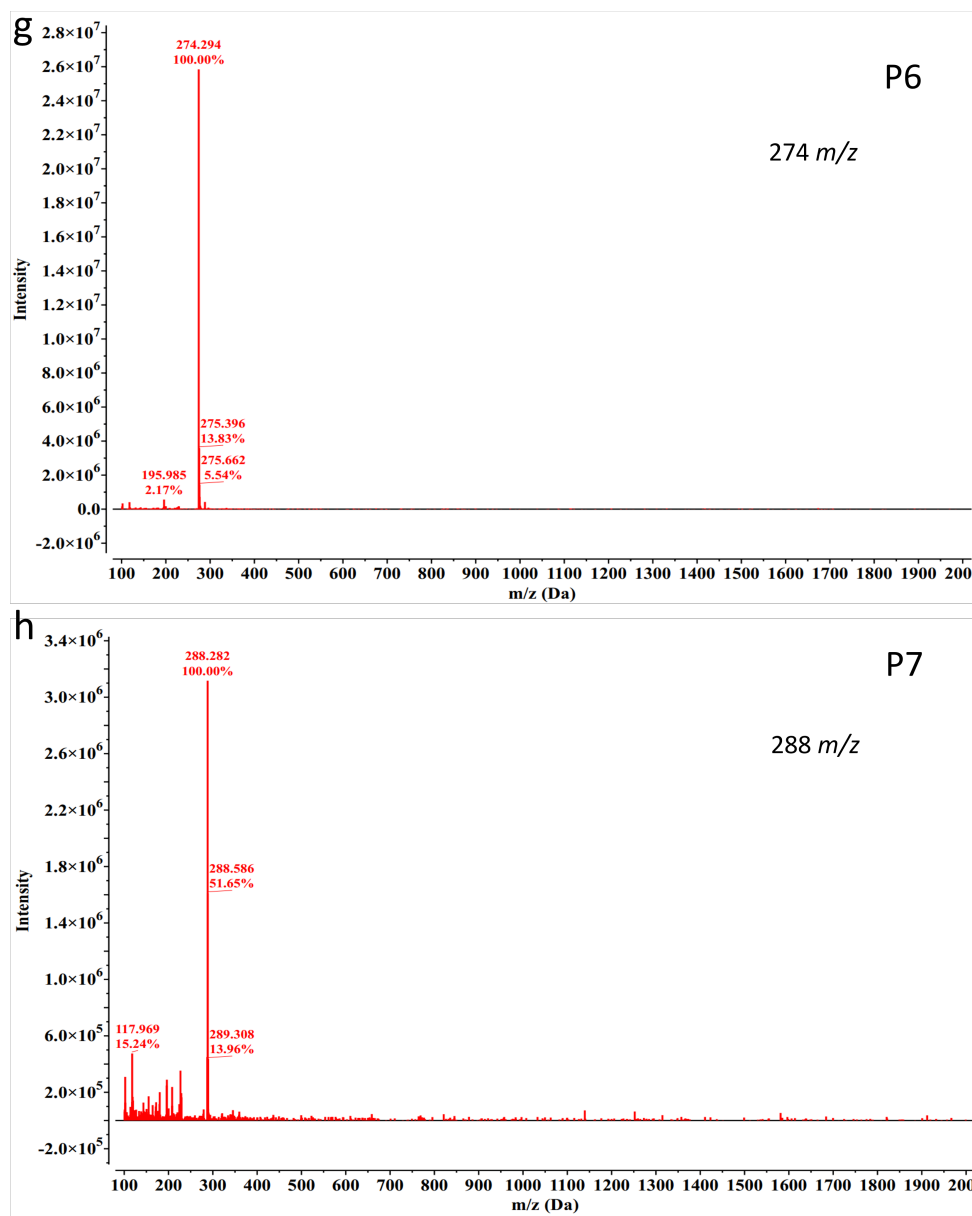


Figure S10: Mass-to-charge ratio ( $m/z$ ) of (a) pure IMC and (b) - (h) UV-degraded products P1 - P7, respectively. Details are summarized in table S2. Note that the substance at RT  $\sim 3.9$  is not a photodegraded product as it is also seen in undegraded IMC (a). The substance might be a process impurity that is unintentionally introduced during the IMC manufacturing process. This substance is chemically stable under light and is not degraded, as its measured UPLC peak intensity in degraded samples and undegraded samples are similar. As such, this substance has no effect on our results. Identification of chemical structures of P1 - P3 were based on known fragmentation pathways of IMC in previously published reports.<sup>2-5</sup> P4-P7 are reaction intermediates and byproducts that have not previously been reported to the best of our knowledge. To determine the chemical structures of these compounds, extensive analyses of authentic compounds are needed to confirm their chemical structures. However, such measurements are outside the scope of this study.



Table S2: Summary of the detected degradation products in UPLC experiments. Each row, from left to right, shows the observed compound, the retention time (RT) found in the UPLC profiles, the mass-to-charge ratio (m/z) measured in the mass spectra for the  $[M-H]^+$  ion, and the specific photodegradation processes where each product was observed. In the right column, S1 and S2 indicate the degradation stage where the product was observed along with the irradiation wavelengths where the product was observed in each stage.

Compounds	RT (min.)	m/z	UV degradation process
IMC	2.30	358	n/a
P1	4.00	314	S1 (254 nm and 365 nm) and S2 (254 nm)
P2	3.00	328	S1 (254 nm and 365 nm) and S2 (254 nm)
P3	1.12	330	S1 (254 nm and 365 nm)
P4	2.04	312	S1 (254 nm and 365 nm) and S2 (254 nm)
P5	3.16	314	S1 (254 nm and 365 nm) and S2 (254 nm)
P6	1.25	274	S2 (254 nm and 365 nm)
P7	1.69	288	S2 (254 nm) and S1 (365 nm)

## References

- (1) Chen, C. Y.; Wang, H.; Shamsabadi, A. A.; Fakhraai, Z. Thermal Stability and Photostability of Highly Confined Molecular Nanocomposites. *Journal of Physical Chemistry B* **2024**, Accepted.
- (2) Temussi, F.; Cermola, F.; DellaGreca, M.; Iesce, M. R.; Passananti, M.; Previtiera, L.; Zarrelli, A. Determination of Photostability and Photodegradation Products of Indomethacin in Aqueous Media. *Journal of Pharmaceutical and Biomedical Analysis* **2011**, *56*, 678–683.
- (3) Zhang, Q.; Chen, P.; Zhuo, M.; Wang, F.; Su, Y.; Chen, T.; Yao, K.; Cai, Z.; Lv, W.; Liu, G. Degradation of Indometacin by Simulated Sunlight Activated CDs-Loaded BiPO<sub>4</sub> Photocatalyst: Roles of Oxidative Species. *Applied Catalysis B: Environmental* **2018**, *221*, 129–139.
- (4) Jiménez, J. J.; Sánchez, M. I.; Pardo, R.; Muñoz, B. E. Degradation of indomethacin in river water under stress and non-stress laboratory conditions: degradation products,

long-term evolution and adsorption to sediment. *Journal of Environmental Sciences* **2017**, *51*, 13–20.

- (5) Wang, F.; Chen, P.; Feng, Y.; Xie, Z.; Liu, Y.; Su, Y.; Zhang, Q.; Wang, Y.; Yao, K.; Lv, W.; Liu, G. Facile Synthesis of N-doped Carbon Dots/G-C<sub>3</sub>N<sub>4</sub> Photocatalyst with Enhanced Visible-Light Photocatalytic Activity for the Degradation of Indomethacin. *Applied Catalysis B: Environmental* **2017**, *207*, 103–113.